International Journal of Energy and Power Engineering
2016; 5(1-1): 48-52
Published online November 5, 2015 (http://www.sciencepublishinggroup.com/j/ijepe)
doi: 10.11648/j.ijepe.s.2016050101.17
ISSN: 2326-957X (Print); ISSN: 2326-960X (Online)

Modeling and Analysis of Leakage Flux and Iron Loss Inside Silicon Steel Laminations

Yong Du*, Wanqun Zheng, Jingjun Zhang

Department of Electrical Engineering, Hebei University of Engineering, Handan, Hebei Province, China

Email address:
duyong_1970@126.com (Yong Du)

To cite this article:
Yong Du, Wanqun Zheng, Jingjun Zhang. Modeling and Analysis of Leakage Flux and Iron Loss Inside Silicon Steel Laminations. *International Journal of Energy and Power Engineering*. Special Issue: Numerical Analysis, Material Modeling and Validation for Magnetic Losses in Electromagnetic Devices. Vol. 5, No. 1-1, 2016, pp. 48-52. doi: 10.11648/j.ijepe.s.2016050101.17

Abstract: This paper investigates the leakage flux and the iron loss generated in the laminated silicon sheets of the core or the magnetic shields of large power transformers. A verification model is well established, and proposed parabolic model (non-saturated region) and hybrid model (saturation region) to simulate the magnetic properties of the silicon steel with different angles to the rolling direction. An efficient analysis method is implemented and validated. The calculated and measured results with respect to the test models are in good agreement.

Keywords: Benchmark Problem 21, Modeling of Silicon Steel Laminations, Arbitrary Anisotropy, Parabolic Model, Hybrid Model

1. Introduction

The iron losses caused in grain-oriented silicon steel sheets of both laminated core and magnetic shields due to the strong leakage magnetic fluxes are highly concerned in very large power transformers. Under operating conditions, the silicon steel sheets performance exhibit non-linearity and anisotropy so that the distributions of the flux density and the iron loss inside each lamination become non-uniform and complex, this usually causes a local overheating. So an exact and quick calculation using three-dimensional finite element method is important [1,2,3]. But if each lamination of core is subdivided into a fine mesh, the number of unknown variables becomes very huge and the calculation is also difficult within an acceptable CPU time. Therefore, a practical modeling method of laminations should be investigated.

Some techniques have been proposed to deal with the iron loss problems about the laminations [4, 5, 6], however, the distributions of the iron loss and the magnetic flux inside the laminations are usually not known clearly. In this paper, based on a benchmark Problem 21—P21^c-M1[7,8], a verification model is proposed, an efficient and practical nonlinear analysis is performed by subdividing only the region near the surface of lamination into a fine mesh, and by modeling the inner part of lamination as a bulk core having anisotropic conductivity. and then proposed parabolic model (non-saturated region) and hybrid model (saturation region) to simulate the magnetic properties of the silicon steel with different angles to the rolling direction. The distributions of the iron loss and the magnetic flux density inside silicon steel laminations are analyzed in details under the different exciting source, and some calculated and measured results of both the magnetic flux density and the iron loss distribution inside the silicon steel sheets are shown.

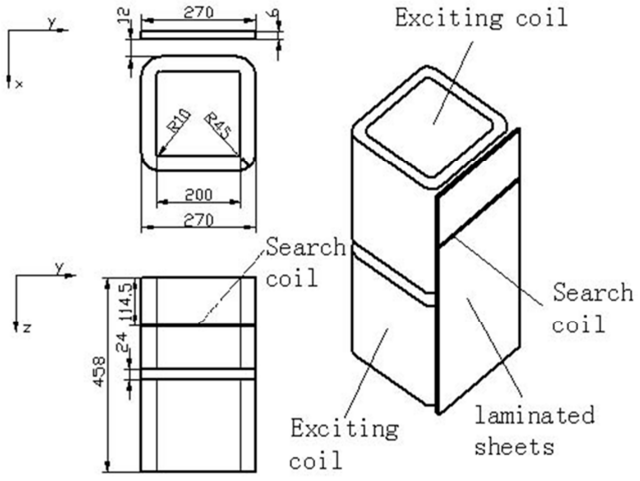

Figure 1. *Model P21^c-M1$^-$.*

2. Model Configuration

2.1. Verification Model

In order to detail the electromagnetic behavior of the grain-oriented silicon steel lamination excited by different applied fields, the original benchmark model of P21^{c}-M1 is simplified, i.e., the solid magnetic steel plate of 10 mm thick is removed so that only the laminated sheets are driven by the exciting source of twin coils (coil 1 and coil 2), which is called Model P21^{c}-M1^{-} [9, 10], as shown in Fig.1.

2.2. Search Coils and Excitations

In the verification model, the grain-oriented silicon steel sheets (30RGH120) are used (total 20 sheets, each sheet is 0.3mm thick). 4 search coils (20 turns for each) are located at the specified positions on the laminated sheets of interest, as shown in Fig.2. The magnetic flux at those specified positions can be obtained by integrating the emf measured from the search coils.

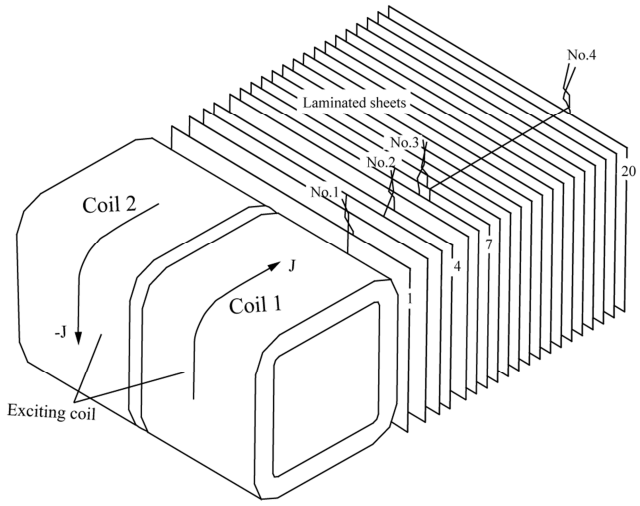

Figure 2. *Located search coils and excitations.*

In order to investigate the magnetic flux and the loss inside the laminations of the verification model under different excitation conditions. There are three testing cases depended on the exciting source, i.e., the exciting current, J, is different in two exciting coils, coil 1 and coil 2 for three cases, as shown in Table1.

Table 1. *Different excitation conditions.*

Cases	Exciting currents (A, rms, 50Hz)	
	in Coil 1	in Coil 2
I	J	-J
II	J	J
III	J	0

Note that the exciting current, J, is ranged from 0A to 25A (rms, 50Hz). The search coils are located at different layers of 20 sheets, and the number of the sheets included in each search coil (e.g., no.1 to no.4) is also different. See Fig.2.

3. Experiments

To simplify the physical model and establish a reasonable computational model, some advance measurements have been done to observe the electromagnetic behavior. The experiments upon the magnetic flux and the loss inside the laminations of the verification model under different excitation conditions have been carried out.

3.1. Average Flux Density Inside Laminated Sheets

The measured results of magnetic flux (or averaged magnetic flux density) passing through the different search coil under the different exciting conditions are shown in Fig. 3.

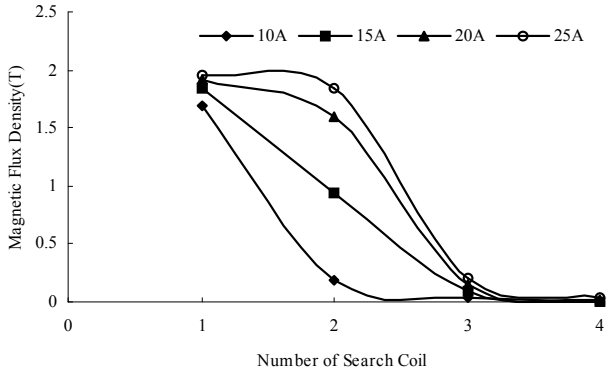

(a) Case I

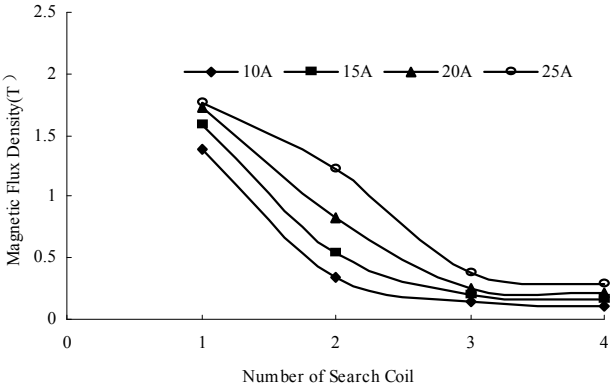

(b) Case II

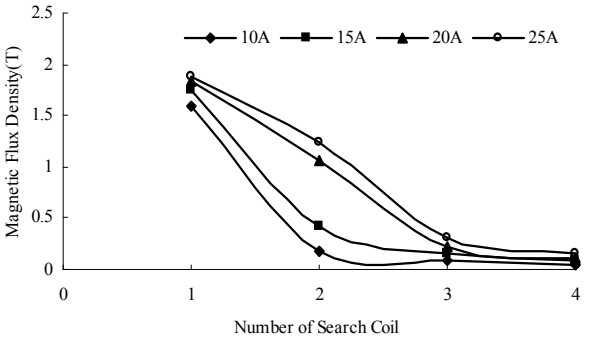

(c) Case III

Figure 3. *Measured average flux density inside laminated sheets under different exciting conditions.*

It can be seen that the averaged magnetic flux density of the laminations closest to the exciting source is considerably high than that far away from the exciting source. And the averaged magnetic flux density will be reduced quickly with the increase of the number of the laminated sheets.

3.2. Total Iron Loss Inside All the Laminated Sheets

The total iron loss inside all the laminated sheets (20 sheets) are also measured at different exciting currents, the measured results are shown in Fig.4.

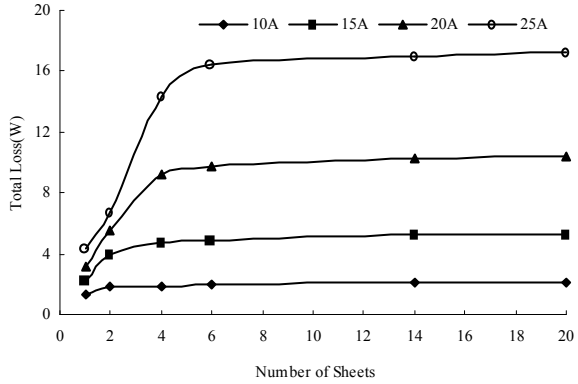

(a) Case I

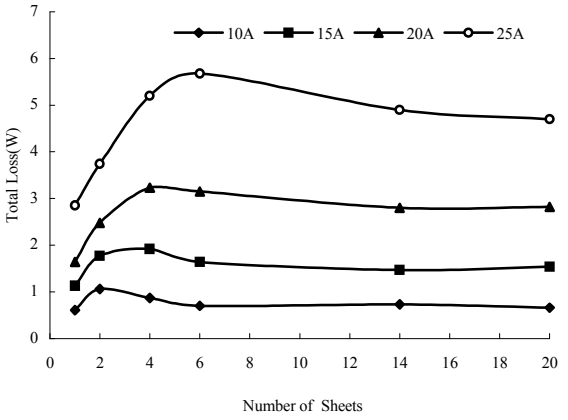

(b) Case II

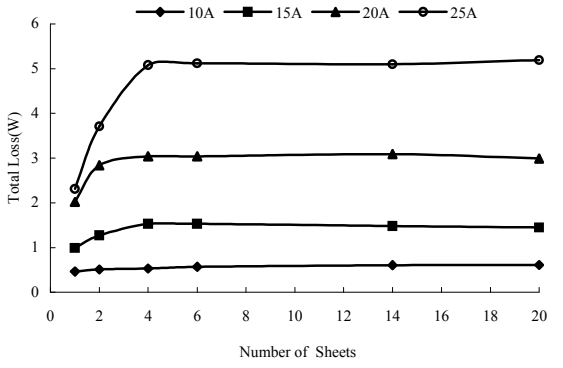

(c) Case III

Figure 4. *Measured iron loss inside laminated sheets under different exciting conditions.*

It can be seen from Fig.4. The total iron loss inside the laminated sheets is also focused on the laminations that closest to the exciting source, and it will be constant with the increase of the number of the laminated sheets.

4. Finite Element Formulation

4.1. The Simplified Computation Model

The experiment results show that the averaged magnetic flux density and the total iron loss within the laminations are quite non-uniform. The eddy currents induced in the laminations by 3-D leakage flux become a real 3-D distribution, especially in the first few laminations closest to the exciting source. In that case the detailed 3-D eddy currents must be investigated.

On the other hand, the magnetic flux density and then the iron loss inside the remained laminations, far away from the exciting source is reduced very quickly.

To simplify the analysis model, the actual silicon steel laminations of the iron core must be simplified on computation, the electromagnetic non-linearity and anisotropy of the laminations should be taken into account. The simplified computation model is shown in Fig.5. In order to simulate the effects of the eddy currents, the first few laminations closest to the exciting source are necessary to model the individual laminations and divided by 0.1 mm thick mesh layers，and the number of the individual lamination models increases with the exciting current increasing. The remaining laminations are modeled as a bulk with the anisotropic material property and divided by 0.9mm thick mesh layers.

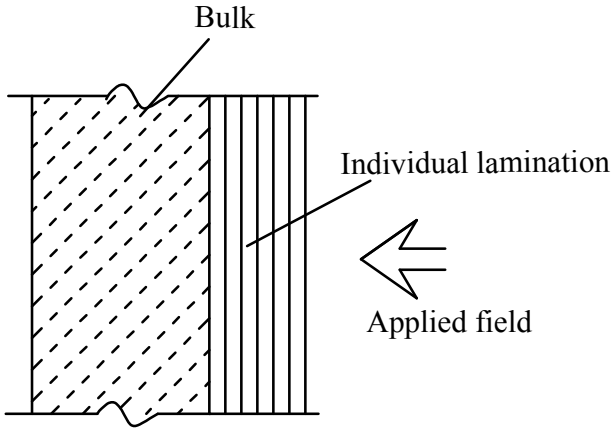

Figure 5. *Simplified computation model.*

4.2. Formulation

The well established $\boldsymbol{T}$-ψ (or expressed as $\boldsymbol{T}$-Ω) method is applied in this simplification of model[11,12], which features the hierarchical element method (based on polynomial orders 1 to 3) and in which the magnetic field is represented as the sum of two parts: the gradient of a scalar potential in non-conducting medium, and an additional vector field represented with vector-edge elements in conducting medium,

described as follows:

1) In the conducting medium, the governing equation is:

$$\nabla\times\left(\frac{1}{\sigma}\nabla\times\boldsymbol{H}\right)+\boldsymbol{\mu}\frac{\partial\boldsymbol{H}}{\partial t}=0 \tag{1}$$

2) In the non-conducting medium, the governing equation is:

$$\nabla\cdot\left[\mu\left(-\nabla\psi+\boldsymbol{H}_s\right)\right]=0 \tag{2}$$

$$\boldsymbol{H}=-\nabla\psi+\boldsymbol{H}_s \tag{3}$$

Where $\boldsymbol{H}_s$ represents the contribution from the exciting source.

4.2. B-H Modeling

The simplest non-linear and anisotropic material model is the elliptical model that uses the properties in the rolling and transverse directions [13]. This model approximately models the material properties in any directions other than the major axes of the material. it derives the permeability in a principal direction directly from the relevant B–H curve based on the magnitude of the applied magnetic field. If a two-dimensional magnetic field with constant magnitude is applied in different directions, the permeability of each principal direction is constant. and, therefore, the vector of the flux density traces an ellipse. However, the new experiment results show that the elliptical model does not provide good accuracy.

For more accurate modeling of the non-linear anisotropic B-H property has been proposed, they are parabolic model (non-saturated region) and hybrid model (saturation region), Through comparing the simulation results that obtained form the elliptic model and the new model with the experiment results, verified that the new model has higher simulated accuracy. In this paper, the new model can be used. They can be basically formulated by (4) and (5) respectively.

$$\frac{B_y^2}{\mu_{y0}^2}+H\frac{B_x}{\mu_{x0}}=H^2 \tag{4}$$

$$\frac{B_y^2}{\mu_{y0}^2}+\frac{1}{2}\left(\frac{B_x^2}{\mu_{x0}^2}+H\frac{B_x}{\mu_{x0}}\right)=H^2 \tag{5}$$

Where parametersμ_{x0} andμ_{y0} are the longitudinal and transverse permeability. The global flux density B is then defined by the following equations:

$$B=H/\sqrt{\left(\cos\phi/\mu_{x0}\right)^2+\left(\sin\phi/\mu_{y0}\right)^2} \tag{6}$$

$$\phi=\arctan\left(\mu_{y0}/\mu_{x0}\tan\tau\right) \tag{7}$$

$$B_Y=B\cdot\sin\phi \tag{8}$$

$$B_x=B\cdot\cos\phi \tag{9}$$

Where ϕ is the angle between the rolling direction and flux density, τ is the angle between the rolling direction and the magnetic field.

The new models require only two curves in the principal directions when we perform the analysis in finite element formulation. In addition to its simplicity, an advantage of the models is that these B–H curves are available directly from the manufacturers.

4.3. Results and Discussion

The measured and calculated total iron loss and flux results are shown in Table 2 and Table 3 respectively. Table 2 and Table 3 show a good agreement between the measured and calculated results for each test case at different exciting currents.

In the further 3-D eddy current analysis, the effect of the different exciting conditions on the total iron loss generated in the laminated sheets is taken into account.

Table 2. *Measured and calculated total loss under different cases.*

Exciting currents (A, rms, 50Hz)	Case I(W)		Case II(W)		Case III(W)	
	Measured	Calculated	Measured	Calculated	Measured	Calculated
10	2.20	2.17	0.66	0.64	0.59	0.58
15	5.30	5.25	1.43	1.39	1.39	1.34
20	10.20	9.96	2.71	2.65	2.99	2.91
25	16.80	15.73	4.72	4.68	5.19	4.97

Table 3. *Measured and calculated total flux inside twenty sheets under different cases.*

Exciting current (A, rms, 50Hz)	CaseI/ (mWb)		CaseII/ (mWb)		CaseIII/ (mWb)	
	Measured	Calculated	Measured	Calculated	Measured	Calculated
10	0.297	0.311	0.357	0.381	0.329	0.323
15	0.444	0.447	0.532	0.569	0.490	0.501
20	0.589	0.594	0.708	0.707	0.652	0.672
25	0.738	0.702	0.886	0.893	0.817	0.832

From Table 2 it can be also seen that the total iron loss of the Case I is about three times of that of the Case III, while, the total iron loss of the Case II is approximately equal to that of Case III. However, the fluxes within 20 sheets for the three cases do not have the same relationship (Table 3). So, there is a complex function relationship between the loss, the fluxes and the exciting sources.

5. Conclusion

A simplified benchmark model involving lamination structures is well established to investigate the iron loss caused by the normal leakage flux, and examine the effects of the eddy currents on the total iron loss. A practical approach, in which the whole solved region is divided into the 3-D and 2-D eddy current sub-regions, is implemented to deal with the lamination configuration and the additional iron loss problems. The electric and magnetic anisotropic properties of the grain-oriented silicon steel are taken into account in the FEM analysis, as well as the magnetic nonlinearity of it according to the parabolic model (non-saturated region) and hybrid model (saturation region).

The distributions of the magnetic flux and the iron loss inside silicon steel laminations are analyzed in detail under different excitation conditions. The simplified analysis method is validated based on the proposed model by comparing the calculated results of the iron losses and the fluxes in sheets.

Acknowledgement

This work was supported by the Youth Science Fund of Hebei Education Department, China, under Grant No. QN20131025 and the National Natural Science Foundation of China, under Grant No. 11272112. This work was also supported by R & D Center, Baoding Electric Co., LTD, China. The Author thanks the all colleagues of R & D Center for their energetic supports and helpful discussions.

References

[1] Du Y, Cheng Z, Zhang J, Liu L, Fan Y, Wu W, Zhai Z, and Wang J, "Additional iron loss modeling inside silicon steel laminations," IEEE International Electric Machines and Drives Conference, pp.826-831, 2009.

[2] Cheng Z, Takahashi N, Forghani B, Du Y, Zhang J, Liu L, Fan Y, Hu Q, Jiao C, and Wang J, "Large power transformer-based stray-field loss modeling and validation," IEEE International Electric Machines and Drives Conference, pp.548-555, 2009.

[3] E. teNyenhuis, R. Girgis, and G. Mechler, "Other factors contributing to the core loss performance of power and distribution transformers," *IEEE Trans. on Power Delivery*, vol., no.4, pp.648-653, October 2001.

[4] L. Krähenbühl, P. Dular, T. Zeidan, and F. Buret, "Homogenization of lamination stacks in linear magnetodynamics," *IEEE Trans. Magn.*, vol. 40, no.2, pp.912-915, March 2004.

[5] K. Muramatsu, T. Shimizu, A. Kameari, I. Yanagisawa, S. Tokura, O. Saito, and C. Kaido, "Analysis of eddy currents in surface layer of laminated core in magnetic bearing system using leaf edge elements," *IEEE Trans. Magn.,* vol. 42, no.4, pp. 883-886, April 2006.

[6] Z. Cheng, N. Takahashi, S. Yang, T. Asano, Q. Hu, S. Gao, X. Ren, H. Yang, L. Liu, and L. Gou, "Loss spectrum and electromagnetic behavior of problem 21 family," *IEEE Trans. Magn.*, vol.42, no.4, pp.1467-1470, 2006.

[7] Z. Cheng, N. Takahashi, B. Forghani, G. Gilbert, J. Zhang, L.Liu, Y. Fan, X. Zhang, Y. Du, J. Wang, and C. Jiao, "Analysis and measurements of iron loss and flux inside silicon steel laminations," *IEEE Trans. Magn*.,45(3): 1222-1225, 2009.

[8] Z. Cheng, N. Takahashi, B. Forghani, L. Liu, Y. Fan, T. Liu, J. Zhang, and X. Wang, "3-D finite element modeling and validation of power frequency multi-shielding effect," *IEEE Trans. Magn.*, vol.48, 243-246, 2012.

[9] Z. Cheng, N. Takahashi, B. Forghani, Y. Du, Y. Fan, L. Liu, and H. Wang, "Effect of variation of B-H properties on both iron loss and flux in silicon steel lamination," *IEEE Trans. Magn.*, vol.47,1346-1349, 2011.

[10] W. Zheng, and Z. Cheng, "An inner-constrained separation technique for 3-D finite-element modeling of grain-oriented silicon steel laminations," *IEEE Trans. Magn.*, vol.48, no.8, pp. 2277-2283, 2012.

[11] Yong Du, Zhiguang Cheng, Zhigang Zhao, Yana Fan, Lanrong Liu, Junjie Zhang, and Jianmin Wang, "Magnetic Flux and Iron Loss Modeling at Laminated Core Joints in Power Transformers," *IEEE Trans. on Applied Superconductivity*, 20(3):1878-1882, 2010.

[12] J.P. Webb and B. Forghani, "A T-Omega method using hierarchal edge elements," IEE Proc.-Sci. Meas. Technol., vol. 142, no. 2, pp.133-141, 1995.

[13] A Di Napoli, and R Paggi, "A model of anisotropic grain-oriented steel," *IEEE Trans. Magn.*, vol. 23, no.5, pp. 1557-1561, July 1983.